Effect of Molecular Weight on the Interfacial Excess, Tension, and Width in a Homopolymer/Binary Polymer Blend System

Jan Genzer*,† and Russell J. Composto

Department of Materials Science and Engineering and Laboratory for Research on the Structure of Matter, The University of Pennsylvania, Philadelphia, Pennsylvania 19104-6272

Received July 8, 1997; Revised Manuscript Received October 16, 1997

ABSTRACT: The interfacial properties of a three-component, two-phase A/B:C blend are investigated to understand the effect of the A and B chain lengths on the interfacial excess of B, z_B^*, the interfacial tension, γ_{ABC}, and the interfacial width, w_{ABC}. The A/B:C components are polystyrene/poly(d_8-styrene-*co*-4-bromostyrene):poly(styrene-*co*-4-bromostyrene), where B and C have 4-bromostyrene mole fractions of 0.154 and 0.177, respectively. Low-energy forward recoil spectrometry (LE-FRES) is used to measure z_B^* as a function of the B volume fraction in the B:C blend, $\phi_{B\infty}$. The experimental z_B^*'s are found to be in excellent agreement with those calculated using the self-consistent field (SCF) model of the A/B:C interface. In addition, the SCF model is used to evaluate γ_{ABC} and the widths for the A/B:C, A/B, and A/C interfaces (*i.e.*, w_{ABC}, w_{AB}, and w_{AC}, respectively). Our results demonstrate that increasing the number of B segments, N_B, greatly increases the magnitude of z_B^*, particularly at low $\phi_{B\infty}$. On the other hand, varying N_A has only a minor effect on z_B^*. Concurrent with the segregation of B, γ_{ABC} and w_{AB} rapidly decrease and increase, respectively, as $\phi_{B\infty}$ initially increases. Upon calculation of the entanglement length, w_e, for each component, w_{AB} is found to approach w_e when $\phi_{B\infty} \approx 0.30$. As a result the mechanical strength of the interface should greatly improve. The optimum amount of B to achieve good compatibilization correlates with the $\phi_{B\infty}$ at which z_B^* is a maximum.

1. Introduction

Blending has proven to be a convenient method to improve and adjust the properties and processability of polymeric materials.[1,2] Polymer blends usually contain two or more components selected such that the principal advantages of one polymer will compensate for deficiencies of the other polymer and *vice versa*. Because of strong chemical incompatibility between most polymer pairs (*i.e.*, large positive interaction parameter, χ), simple blending usually results in macroscopically phase-separated materials with little practical use. For such a blend, the bulk properties are strongly influenced by the interfacial properties between immiscible phases. The interfacial tension and width are two critical parameters that characterize the interface. For example, the interfacial tension controls the phase morphology. Due to strong incompatibility, the interfacial tension is typically quite high,[3] resulting in morphologies with widely-separated, large phases. In addition, narrow interfacial widths result in poor adhesion and low fracture toughness because of the limited interpenetration across the interface.[4]

Compatibilizers added to these immiscible polymer blends can overcome the above deficiencies in several ways. First, they usually reduce the interfacial tension which leads to a fine dispersion of the minority phase. In addition, compatibilizers broaden the interfacial width thereby providing improved interfacial stress transfer and adhesion. Third, compatibilizers can stabilize the minority phase by slowing down its growth during processing. In practice, these effects will occur to various degrees depending on the particular compatibilizer. Other properties, such as rheology, can also be modified and controlled. Typical compatibilizers include block copolymers, graft copolymers, reactive/functional copolymers, in-situ grafting agents, *etc.*[1,2,5] In particular, block copolymers[4,6] and graft copolymers[7] can greatly improve the mechanical properties and decrease the interfacial tension between immiscible polymer pairs, A/C. For example, the fracture toughness of a polystyrene (PS)/poly(methyl methacrylate) (PMMA) interface was increased by a factor up to 50 upon adding a P(S-*b*-MMA) block copolymer to the interface.[8] Recently, random copolymers (A-*co*-C) were found to also improve the fracture toughness of A/C systems.[9]

There are several limitations associated with using block copolymers as compatibilizers. First, block copolymers are expensive compared to most commercial polymers. Second, if not applied directly to the interface, block copolymers have to diffuse to the interface and therefore their effectiveness can be limited by kinetics. Also, at concentrations greater than the critical micelle concentration (cmc), block copolymers form micelles. In many cases, the cmc can be as small as 1%. The formation of micelles thus limits the availability of block copolymers which can span the A/C interface. In addition, copolymer micelles usually tend to segregate at the A/C interface which reduces the "effective space" for compatibilization. On the other hand, homopolymers (or random copolymers) can be very attractive compatibilizing agents because of their lower cost. Indeed, recent theoretical[10−12] and experimental[13,14] studies have demonstrated that homopolymers can be used as effective compatibilizing agents. Recently, Helfand[11] and Yoon and co-workers[12] calculated that the interfacial properties of an immiscible A/C pair can be improved by the addition of component B, which is miscible with C but not with A. Using the self-consistent field (SCF) method, these studies demonstrated that B segregates to the A/B:C interface, if χ_{AB}

† Current address: Department of Materials, University of California at Santa Barbara, Santa Barbara, CA 93106.

S0024-9297(97)00993-5 CCC: $15.00
Published on Web 01/22/1998

$< \chi_{AC}$. As B adsorbs to the A/B:C interface, the interfacial tension, γ_{ABC}, was found to decrease whereas the interfacial width, w_{ABC}, increased.

In these models,[11,12] the free energy density of the system is governed solely by the enthalpy of mixing. Therefore these models are only valid in the infinite molecular weight limit where the entropy of mixing is neglected. Moreover, these models are limited to systems having $\chi_{BC} < 0$. The former simplification prevents direct experimental testing of the model whereas the latter greatly limits the number of polymer systems to which these models can be applied. To overcome these difficulties, we have modified the SCF model to include the contribution of the entropy of mixing to the free energy of the system.[15] This model can then be tested on finite molecular weight systems and B:C pairs having $\chi_c > \chi_{BC} > 0$, where χ_c is the critical value of χ_{BC}. An important result from this modified model is that the A/B:C interfacial properties depend strongly on the number of B segments, N_B, but rather weakly on N_A.

In an earlier study, low-energy forward recoil spectrometry (LE-FRES) was used to measure z_B^* as a function of B volume fraction in the B:C mixture, $\phi_{B\infty}$, for the case where $\chi_{AB} < \chi_{AC}$.[16] These measurements provided the first experimental detection of segregation at the homopolymer/binary polymer blend interface. In subsequent experiments neutron reflectivity (NR) was used to determine the shape of the polymer volume fraction profiles.[17] These NR measurements also provided a direct measure of the interfacial width between the A and B:C phases. In the present study, we revisit the issue of interfacial segregation using a slightly different blend system designed to more rigorously test the SCF model. One objective is to investigate the effect of N_A and N_B on the A/B:C interfacial properties. As before, LE-FRES is used to measure z_B^*. In contrast to previous studies, z_B^* is measured over a much broader range of $\phi_{B\infty}$. We find that an increase in N_B leads to a dramatic increase in z_B^*, a smaller γ_{ABC}, and a larger w_{ABC}. However, an increase in N_A by *ca.* 1.5 orders of magnitude does not measurably change the interfacial properties. Qualitatively and quantitatively, the behavior of z_B^* as a function of $\phi_{B\infty}$ is in excellent agreement with SCF predictions.

2. Experiment

2.1. Materials and Sample Preparation. Similar to previous experiments, the two-phase, three-component system consists of polystyrene, PS, and blends of two miscible random copolymers of poly(styrene-*co*-4-bromostyrene), $dPBr_xS$ and PBr_yS, having $x = 0.154$ (or $x = 0.157$) and $y = 0.177$ mole fractions of 4-bromostyrene (4-BrS), respectively. The random copolymers were prepared by brominating d_8-PS and normal PS, respectively, using the procedure of Kambour and coworkers.[18] The values x and y were chosen such that the PS/$dPBr_xS$ and PS/PBr_yS pairs were immiscible. One of the drawbacks of the system studied in refs 16 and 17 was the partial miscibility of the B component in the A phase. This complicated the comparison of the experimental and calculated volume fraction profiles of B. To minimize the solubility of B and C in A, the 4-BrS mole fraction in B and C was increased relative to B and C in refs 16 and 17. By choosing x to be slightly less than y, the interaction parameter between $dPBr_xS$ and PS was tuned and designed to be smaller than that between PBr_yS and PS (*i.e.*, $\chi_{AB} < \chi_{AC}$). In addition, the difference between x and y was small enough to guarantee complete miscibility between $dPBr_xS$ and PBr_yS at all compositions studied. The polymer characteristics are listed in Table 1. To simplify the nomenclature, PS, $dPBr_xS$, and PBr_yS are referred to as A, B, and C, respectively. Because the 4-BrS mole fractions in B1 and B2 are nearly equal, the values of χ_{AB}, χ_{AC}, and χ_{BC} are taken to be the same for the two systems.

Samples were prepared by spin-coating toluene solutions of B:C mixtures on silicon wafers previously etched for 10 min in a 7% v/v HF/water solution. The samples were then dried in a vacuum oven for *ca.* 12 h at 90 °C. A top film was spin-coated on a glass slide from a toluene solution of A, scored around the edges, floated on a deionized water bath, and picked up with a B:C/silicon sample. These bilayers were again dried in a vacuum oven for 12 h at 90 °C. Film thicknesses determined by ellipsometry were *ca.* 600−1000 and 2000−3000 Å for the A and B:C films, respectively. The samples were then annealed at 181 °C. The volume fractions of the B component were determined in both the as-cast and annealed samples using LE-FRES.

2.2. Low-Energy Forward Recoil Spectrometry (LE-FRES). The LE-FRES measurements were carried out on a Model 5SDH Pelletron tandem accelerator (National Electrostatic Corp., WI), interfaced with a custom-designed scattering chamber at the ion beam facility of the Laboratory for Research on the Structure of Matter at the University of Pennsylvania. The technique has been described elsewhere.[19] Briefly, in LE-FRES, a monoenergetic beam of 2.0 MeV $^4He^+$ ions impinges on a sample at an angle of 75° with respect to the sample normal. As a result of the interactions of He ions with the atoms in the sample, the light nuclei, such as H and D, recoil from the sample and travel toward a detector which is placed at an angle of 150° with respect to the incident beam. In addition to the recoiling D and H nuclei, helium atoms are forward scattered from the heavier carbon and silicon atoms in the polymer film and substrate, respectively. To prevent the helium signal from masking the hydrogen and deuterium signals, a 7.5 μm thick Mylar stopper foil is placed before the detector. Multiple scattering of the incident and recoiled ions with the sample nuclei is the main cause of resolution loss below the surface.[19] Using standards, the depth resolution was *ca.* 500 Å at a depth of 1000 Å beneath the sample surface. The resultant LE-FRES spectrum of recoiled yield versus detected energy is then converted to a depth profile of the D and H nuclei.

3. Results

3.1. Experiment. Previously, we observed that the A/B:C interface was enriched with the B component if $\chi_{AB} < \chi_{AC}$.[16,17] As a result of B segregation, the interfacial properties such as the interfacial tension and width were modified. One result of our SCF calculations was that the A/B:C interfacial properties were controlled strongly by the number of polymer segments.[15] In this paper we will investigate the effect of N_A and N_B on z_B^*. Figure 1 shows the B1 volume fraction profile in system Ia before (open circles) and after (closed circles) annealing for 30 days at 181°C. In the as-cast sample, $\phi_{B1\infty}$ is uniformly 0.392 throughout the B:C blend indicating that B1 does not segregate appreciably during spin coating. After the sample is annealed, a small excess of B1 at the interface is detected, as depicted by the shaded area in Figure 1. To conserve B1 in the thin film, $\phi_{B1\infty}$ decreases to 0.326. Figure 1 also shows that B1 is slightly miscible (*ca.* 0.07) in A1. Thus, although the B1−A1 enthalpic repulsion is strong, the entropy of mixing term is large enough to favor partial miscibility. The underlying reason for this miscibility is partly due to the low molecular weight of B1.

Figure 2 shows the B2 volume profile for system Ib before (open circles) and after (closed circles) annealing for 30 days at 181 °C. As in Figure 1, B2 is uniformly distributed throughout the as-cast B2:C blend, having a $\phi_{B2\infty}$ of 0.400. After the sample is annealed, $\phi_{B2\infty}$

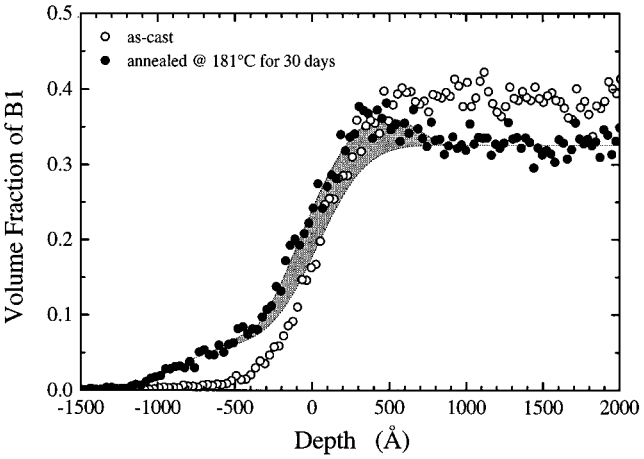

Figure 1. Volume fraction profile of B1 determined by LE-FRES for the A1/B1:C sample as-cast (open circles) and after annealing for 30 days at 181 °C (closed circles). The bulk volume fractions of B1 are 0.392 (as-cast) and 0.326 (annealed). The interface between A1 and B1:C defines the origin of the depth scale. The shaded area represents the interfacial excess of B1, z_{B1}*.

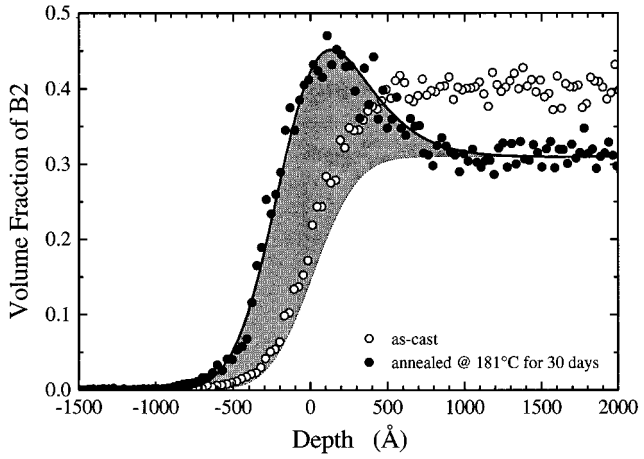

Figure 2. Volume fraction profile of B2 determined by LE-FRES for the A1/B2:C sample as-cast (open circles) and after annealing for 30 days at 181 °C (closed circles). The bulk volume fractions of B2 are 0.400 (as-cast) and 0.310 (annealed). The interface between A1 and B2:C defines the origin of the depth scale. The thick solid line is the volume fraction profile calculated using SCF and corrected for the instrumental resolution of LE-FRES. The shaded area represents the interfacial excess of B2, z_{B2}*.

decreases to 0.310 because of the large interfacial excess of B2 (*i.e.*, shaded area in Figure 2). Because N_B is now 6333 (almost two times larger than in B1), the B component is no longer soluble in A1. More importantly, this increase in N_B results in nearly a factor of 3 increase in z*, where z_{B1}* and z_{B2}* are 65 and 172 Å, respectively. In Figure 2, the thick solid line represents the B2 profile calculated from the SCF model. To correct for instrumental resolution, the SCF profile was convoluted with Gaussian functions having full width at half maximums that increased linearly from 400 Å at the sample surface to 650 Å at a depth of 2000 Å.[20]

Using volume fraction profiles such as those shown in Figures 1 and 2, z_B* was measured for a wide range of $\phi_{B\infty}$. Figure 3 shows z_{B1}* (open circles) and z_{B2}* (closed circles) as a function of $\phi_{B\infty}$ for systems Ia and Ib, respectively. For both systems, the general behavior of z_B* *vs* $\phi_{B\infty}$ is similar. Namely, at small values of $\phi_{B\infty}$, z_B* increases very rapidly, reaches a maximum at a moderate $\phi_{B\infty}$ and decreases to 0 as $\phi_{B\infty}$ approaches unity. In refs 16 and 17, this behavior could only be surmised because of the limited range of $\phi_{B\infty}$. Figure 3 also shows that the magnitude of z_B* at intermediate values of $\phi_{B\infty}$ is significantly larger for system Ib. Recalling that χ_{AB}, χ_{AC}, and χ_{BC} are essentially the same for both systems, the larger N_B in system Ib is mainly responsible for the higher values of z_{B2}*.

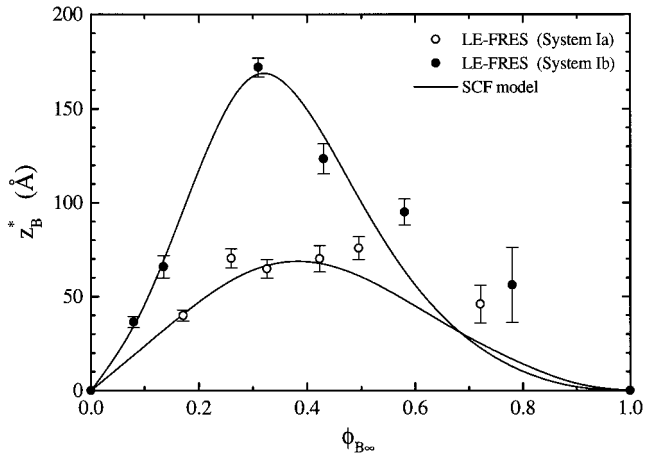

Figure 3. Interfacial excess of B1 (open circles) and B2 (closed circles), z_B*, for systems Ia and Ib as a function of bulk volume fraction, $\phi_{B\infty}$. z_B* is measured by LE-FRES and samples are annealed for 30 days at 181 °C. The solid lines are the results obtained from the SCF model using the numbers of segments listed in Table 1 and the interaction parameters given in the text.

Table 1. Polymer Characteristics[a]

symbol	polymer	N[b]	p.i.	source
A1	PS	3844	1.06	Pressure Chemical
A2	PS	192192[c]	1.20	Pressure Chemical
B1	$dPBr_{0.154}S$	3682	1.05	Polymer Laboratories[d]
B2	$dPBr_{0.157}S$	6333	1.09	Polymer Laboratories[d]
C	$PBr_{0.177}S$	3996	1.06	Pressure Chemical[e]

[a] N and p.i. are the number of segments and the polydispersity index of the polymers, respectively. [b] Calculated for a segmental volume of dPS ($v_{0,dPS} = 1.645 \times 10^{-22}$ cm^3). [c] Based on the nominal molecular weight of a PS standard of 2×10^7 g/mol measured by light scattering in benzene at 25 °C (as reported by vendor). [d] Supplied as dPS. [e] Supplied as PS.

Table 2. A/BC Systems[a]

system	polymer A	polymer B	polymer C
Ia	A1	B1	C
Ib	A1	B2	C
IIa	A2	B1	C
IIb	A2	B2	C

[a] For the polymer characteristics see Table 1.

In addition to the effect of N_B, we have also investigated the effect of N_A on the interfacial properties of the A/B:C interface. These experiments were carried out on systems IIa and IIb, whose characteristics are given in Tables 1 and 2. As for system I, LE-FRES was used to determine the B component volume fraction profiles for samples annealed for 30 days at 181 °C. These profiles of B were then used to determine z_{B1}* and z_{B2}* in systems IIa and IIb, respectively. Figure 4 shows z_{B1}* (open circles) and z_2* (closed circles) as a function of $\phi_{B\infty}$. For systems IIa and IIb, the general behavior of z_B* *vs* $\phi_{B\infty}$ is the same as previously observed for systems Ia and Ib. Namely, at small $\phi_{B\infty}$, z_B* increases very rapidly, reaches a maximum at a moderate $\phi_{B\infty}$, and decreases to 0 as $\phi_{B\infty}$ approaches 1. The

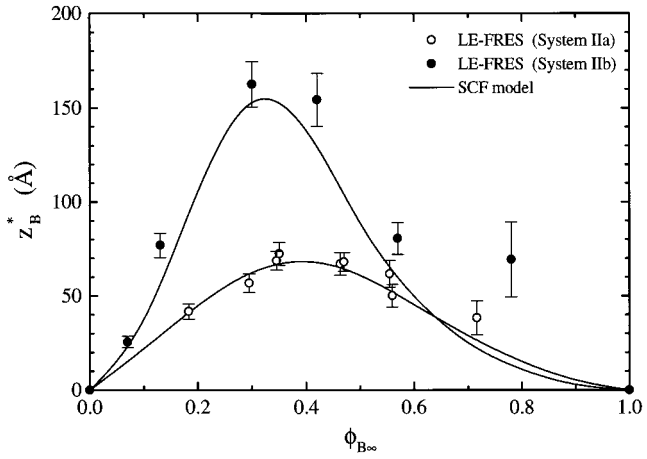

Figure 4. Interfacial excess of B1 (open circles) and B2 (closed circles), z_B*, for systems IIa and IIb as a function of bulk volume fraction, $\phi_{B\infty}$. z_B* is measured by LE-FRES and samples are annealed for 30 days at 181 °C. The solid lines are the results obtained from the SCF model using the numbers of segments listed in Table 1 and the interaction parameters given in the text.

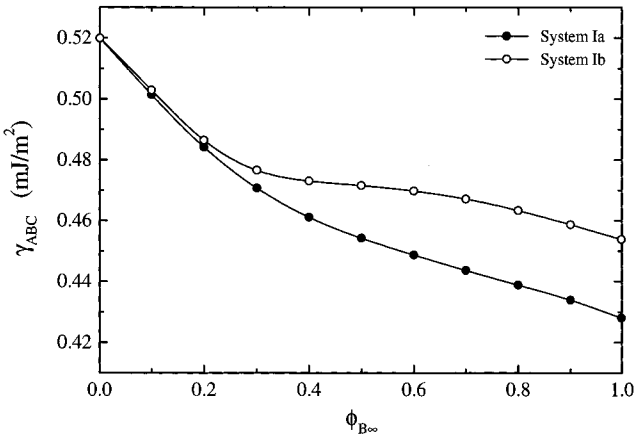

Figure 5. Dependence of the interfacial tension, γ_{ABC}, on the bulk volume fraction of B in the B:C mixture, $\phi_{B\infty}$, for systems Ia (closed circles) and Ib (open circles) calculated using the SCF model and the Gibbs adsorption equation (for details see Appendix A2), respectively.

main difference between z_{B1}* and z_{B2}* is the magnitude of z_B* at moderate values of $\phi_{B\infty}$. As discussed earlier this difference is mainly due to the different values of N_B.

A brief comparison of Figures 3 and 4 reveals that the values of z_B* for systems Ia and IIa are practically equal. The same conclusion holds for the z_B*'s in systems Ib and IIb. These observations show that N_B has a strong effect on z_B* whereas N_A does not greatly influence interfacial segregation. These experimental results are reinforced by SCF calculations which are shown as solid lines in Figures 3 and 4.

3.2 SCF Model. The measured z_B*'s are compared with those predicted by a SCF model. In addition, this model is used to calculate the A/B:C interfacial tension, γ_{ABC}, and width, w_{ABC}. Because the model determines the volume fraction profiles for each component, the interfacial overlap between the A/B, w_{AB}, and A/C, w_{AC}, phases can be found. The details of the model are found elsewhere.[15] Briefly, the A/B:C system is described by seven input parameters, including the number of segments for polymers A, B, and C (N_A, N_B, and N_C), the A−B, A−C, and B−C segment interaction parameters (χ_{AB}, χ_{AC}, and χ_{BC}), and the B volume fraction in B:C ($\phi_{B\infty}$). The values of N_A, N_B, and N_C are found in Table 1.[21] The value of $\chi_{BC} = 3.88 \times 10^{-4}$ is determined from the mutual diffusion coefficient (see Appendix A1). In contrast to our previous approach,[16,17] the values of χ_{AB} and χ_{AC} are allowed to vary to produce the best fits to the experimental z_B*. It is important to note that only one value of χ_{AB} (=2.84×10^{-3}) and χ_{AC} (=3.71×10^{-3}) was used for all the SCF calculations. These values are only slightly different from those previously reported (*i.e.*, $\chi_{AB} = 2.94 \times 10^{-3}$ and $\chi_{AC} = 3.61 \times 10^{-3}$ for $x = 0.154$ and $y = 0.177$, respectively).[22,23] Because of the small difference in the 4-BrS mole fractions of B1 and B2 (*cf.* Table 1), the same values of χ_{AB}, χ_{AC}, and χ_{BC} are used for systems Ia and Ib. Figure 2 shows that the SCF volume fraction of B2 (thick solid line) is in excellent agreement with the experimental data (solid circles). Using the same interaction parameters, similar agreement is found for all other profiles measured. It is quite remarkable that the experimental (circles) and calculated (lines) values of z_B* for each system shown in Figures 3 and 4 are in such excellent agreement over a wide range of $\phi_{B\infty}$. Because z* is small and superimposed on a high background of $\phi_{B\infty}$, the z*'s measured at high $\phi_{B\infty}$ have a higher experimental error than those at low $\phi_{B\infty}$. This may account for the poorer agreement between experiment and SCF at high $\phi_{B\infty}$.[24]

The interfacial tension, γ_{ABC}, is calculated for systems Ia and Ib by two methods. For Ia, γ_{ABC} is evaluated from the SCF model by integrating the incompressibility term, Δw, in the mean-field potential[15]

$$\gamma_{ABC} = k_B T \rho_0 \int_{-\infty}^{\infty} \Delta w(x)\, dx \qquad (1)$$

where k_B is Boltzmann's constant, T is absolute temperature, and ρ_0 is the lattice density. The incompressibility term $\Delta w(x)$ is given by[15]

$$\Delta w(x) = \zeta[1 - \sum_k \phi_k(x)] \qquad (2)$$

where ζ is a parameter proportional to the bulk compressibility of the mixture.[3] Although eqs 1 and 2 produce reasonable results for Ia (see discussion below), the γ_{ABC} values for Ib at intermediate $\phi_{B\infty}$ are unrealistically low (*i.e.*, less than γ_{AC} and γ_{AB}!).[25] To overcome this problem, γ_{ABC} for Ib is determined from the Gibbs adsorption equation (GAE) following the procedure of Norton *et al.*[26] The GAE method is described in Appendix A2. In addition, the GAE approach was used to determine γ_{ABC} for system Ia and found to be in excellent agreement with the SCF results.

Figure 5 shows the calculated γ_{ABC} as a function of $\phi_{B\infty}$ for systems Ia (closed circles) and Ib (open circles) at 181 °C. For Ia, γ_{ABC} monotonically decreases from 0.520 to 0.428 mJ/m^2 as the system progresses from a "pure" A1/C to a "pure" A1/B1 interface. As $\phi_{B\infty}$ increases from 0 to 0.3, γ_{ABC} decreases relatively rapidly; however, beyond $\phi_{B\infty} \approx 0.3$, γ_{ABC} decreases more slowly. Similar behavior is observed for system Ib although the transition near $\phi_{B\infty} \approx 0.3$ is accentuated because γ_{ABC} tends to level off for $\phi_{B\infty} > 0.4$. This plateau-like region is due to the higher value of the pure A1/B2 interfacial tension (0.454 mJ/m^2) relative to A1/B1 in system Ia (0.428 mJ/m^2). For $\phi_{B\infty} < 0.3$, the magnitude that γ_{ABC} decreases in both Ia and Ib is similar. Thus, at low $\phi_{B\infty}$ the efficiency of lowering γ_{ABC} is nearly equivalent for

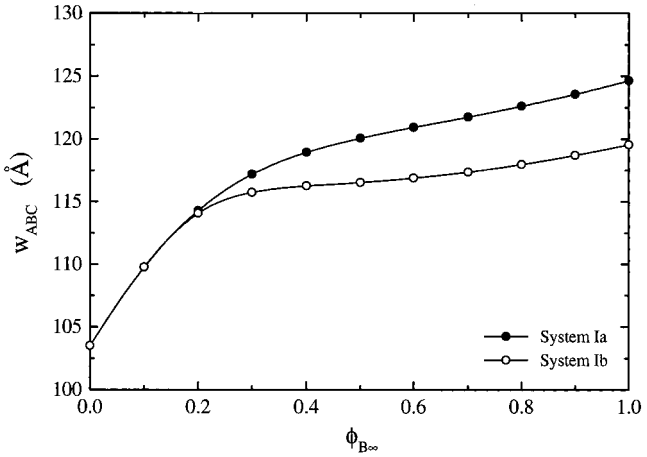

Figure 6. Dependence of the interfacial width, w_{ABC}, on the bulk volume fraction of B in the B:C mixture, $\phi_{B\infty}$, for systems Ia (closed circles) and Ib (open circles) calculated using the SCF model.

both N_B's studied. The physical interpretation of the dependence of γ_{ABC} on $\phi_{B\infty}$ is given in section 4.

The SCF interfacial width, w_{ABC}, is plotted in Figure 6 for systems Ia (closed circles) and Ib (open circles). Comparison of Figure 6 with Figure 5 reveals that the behavior of w_{ABC} with $\phi_{B\infty}$ mirrors that of γ_{ABC}. Namely, in Ia w_{ABC} increases gradually from 103.5 to 124.6 Å as the system moves from the A1/C interface to the A1/B1 interface, respectively. w_{ABC} increases quite rapidly as $\phi_{B\infty}$ initially increases and then more gradually for $\phi_{B\infty} > 0.3$. In Ib, w_{ABC} qualitatively follows the same trend as in Ia in the region $\phi_{B\infty} < 0.3$. For $\phi_{B\infty} > 0.3$, w_{ABC} increases more slowly, reaching a value of 119.6 Å.

To further understand the behavior of w_{ABC}, the interfacial widths of component A with B, w_{AB}, and of A with C, w_{AC}, are plotted in parts a and b of Figure 7, respectively, for systems Ia (closed circles) and Ib (open circles). For Ia, Figure 7a illustrates that w_{AB} rises rapidly as $\phi_{B\infty}$ increases from 0 to *ca.* 0.3 and then more slowly as $\phi_{B\infty}$ continues to increase. For Ib, w_{AB} initially increases more rapidly than in Ia, but then reaches a plateau between 0.3 and 0.6 before increasing again. Note that the difference between w_{AB} in Ia and Ib is significant at low $\phi_{B\infty}$ (<0.3). For example, at $\phi_{B\infty} \approx 0.2$, w_{AB} for Ib is about 24% greater than its corresponding value for Ia. These observations indicate that at low $\phi_{B\infty}$ the overlap between A and B will increase more strongly for systems with higher N_B. Whereas w_{AB} increases with $\phi_{B\infty}$, Figure 7b demonstrates that w_{AC} initially decreases strongly and then near $\phi_{B\infty} \approx 0.3$ starts to decrease at a much slower rate as $\phi_{B\infty}$ approaches 1. Recall that w_{ABC} is nearly independent of N_B for $\phi_{B\infty} < 0.3$ (*cf.* Figure 6). Therefore, the increase in w_{AB} at large N_B must be compensated by the decrease in w_{AC}.

The SCF z_B*'s for systems I and II (Figures 3 and 4) are found to be in excellent agreement with the measured values. Moreover, the SCF values of the interfacial tension and widths for system I are given in Figures 5, 6, and 7. For completeness, the SCF calculations of γ_{ABC} and w_{ABC}, along with z_B* are presented in Table 3 for system II. Qualitatively, γ_{ABC} and w_{ABC} have the same functional dependence on $\phi_{B\infty}$ for both systems I and II. A quantitative comparison between Ia and IIa reveals that z_B* and w_{ABC} are slightly smaller, and γ_{ABC} is slightly larger in the system which has the larger N_A.

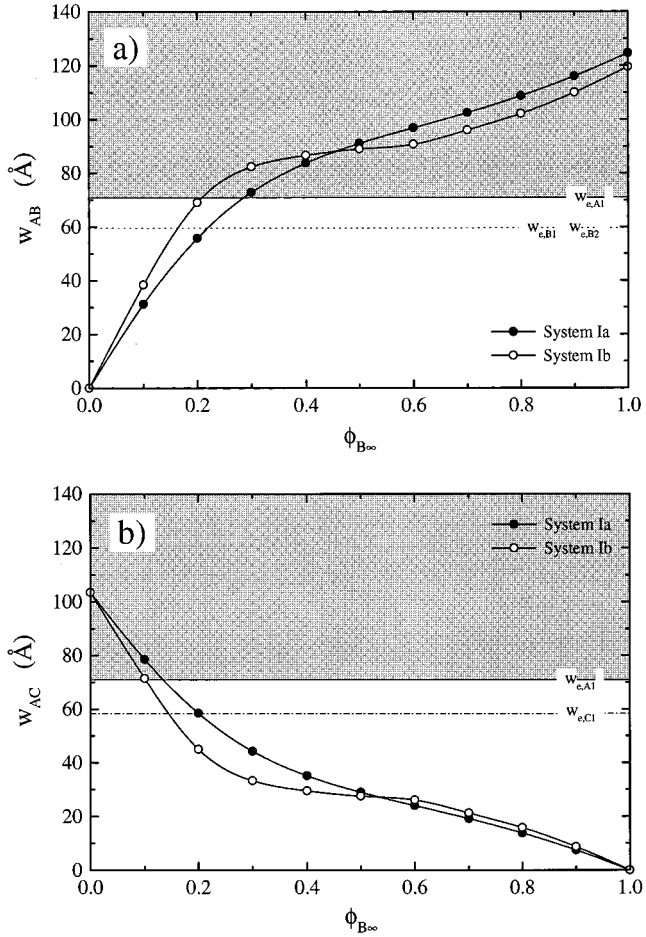

Figure 7. Dependence of (a) the interfacial overlap between A1 and B1, w_{AB}, in system Ia (closed circles) and A1 and B2 in system Ib (open circles) and b) the interfacial overlap between A1 and C, w_{AC}, in system Ia (closed circles) and system Ib (open circles) on the bulk volume fraction of B, $\phi_{B\infty}$. The interfacial widths were calculated from the SCF model. The horizontal lines denote the average entanglement length in A (solid line), B (dotted line), and C (dash-dotted line).

Table 3. Interfacial Properties Determined from the SCF Model

	system IIa (A2/B1:C)[a]			system IIb (A2/B2:C)[a]		
$\phi_{B\infty}$	z_{B1}* (Å)	γ_{ABC} (mJ/m^2)	w_{ABC} (Å)	z_{B2}* (Å)	γ_{ABC}[b] (mJ/m^2)	w_{ABC} (Å)
0.0	0	0.579	96.0	0	0.579	96.0
0.1	22.2	0.556	101.0	37.8	0.557	101.1
0.2	44.8	0.538	104.7	105.6	0.541	104.6
0.3	62.4	0.525	107.1	152.8	0.531	106.1
0.4	68.2	0.516	108.5	137.9	0.526	106.5
0.5	60.8	0.509	109.5	88.7	0.522	106.7
0.6	45.3	0.503	110.1	49.8	0.519	106.9
0.7	28.8	0.499	110.8	25	0.516	107.3
0.8	15.2	0.494	111.4	11	0.513	107.8
0.9	5.4	0.489	112.2	3	0.511	108.4
1.0	0	0.484	112.9	0	0.508	109.2

[a] For the polymer characteristics see Table 1. [b] Calculated using the GAE approach (see Appendix A2 for details).

A similar relationship is observed upon comparing Ib with IIb. Because increasing N_A by a factor of *ca.* 50 has only a minor effect on the interfacial properties, we will restrict the discussion section mainly to systems Ia and Ib and focus on the influence of N_B.

4. Discussion

In this section we provide a physical interpretation of the results presented in the previous part of this

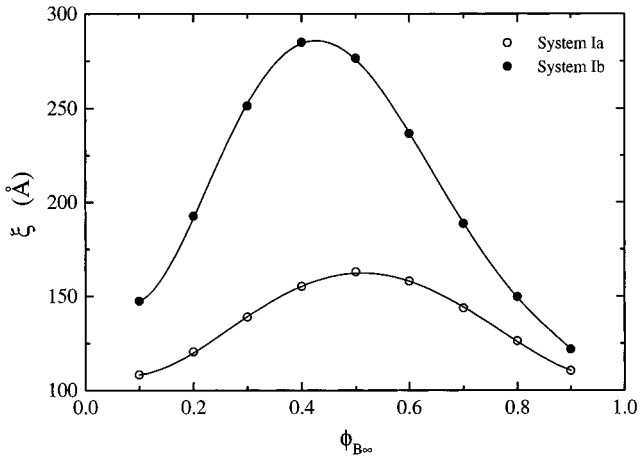

Figure 8. Dependence of the correlation length, ξ, on the bulk volume fraction of B in the B:C mixture, $\phi_{B\infty}$, for systems Ia (open circles) and Ib (closed circles). The values of ξ were determined from the SCF volume fraction profiles using the procedure outlined in Appendix A3.

paper. The thermodynamic driving forces governing the origin of the interfacial excess of B have been discussed previously.[15] Briefly, upon addition of B to a strongly immiscible A/C system, the B component will segregate to the A/B:C interface if $\chi_{AB} < \chi_{AC}$. Thus, the system free energy is lowered by replacing the more unfavorable A−C contacts with less unfavorable A−B ones. At low $\phi_{B\infty}$, this rearrangement of polymers at the interface results in a strong increase of z_B* and decrease in γ_{ABC} as $\phi_{B\infty}$ initially increases. Upon further increase of $\phi_{B\infty}$, the B interfacial excess continues to increase until the enthalpic gain associated with replacing the A−C contacts by the A−B ones is outweighed by the energy cost for removing B from the interfacial region where the C concentration is quite low. The maximum z_B* corresponds to a $\phi_{B\infty}$ at which these two trends are balanced. In Figures 3 and 4, z_{B1}* and z_{B2}* have maxima at $\phi_{B1\infty} \approx 0.38$ and $\phi_{B2\infty} \approx 0.32$, respectively. Thus, upon increasing N_B the maximum z_B* not only increases (*i.e.*, $z_{B2}^* \approx 2.5 z_{B1}^*$) but the $\phi_{B\infty}$ corresponding to this maximum shifts to lower values. This shift can be attributed to an increase in the entropic penalty associated with removing a large molecule from the B:C mixture and putting it at the interface.

As discussed in ref 15, z_B* is expected to increase as N_B increases for the following reason. For binary polymer blends in contact with air, previous studies (e.g., refs 26 and 27) have shown that the surface excess of the segregating polymer scales with the blend correlation length, ξ. Far from the two-phase region, ξ is nearly equal to the radius of gyration of the segregating polymer. However, as the phase boundary is approached, ξ increases rapidly and eventually diverges.[27,28] If air is replaced by polymer A (as in our case), the previous argument can also describe the segregation of B at the A/B:C interface. Thus, the behavior of z_B* as a function of $\phi_{B\infty}$ should mirror that of the B:C correlation length. Figure 8 shows the variation of ξ with $\phi_{B\infty}$ for systems Ia (open circles) and Ib (closed circles). The values of ξ were determined from the SCF volume fraction profiles using the procedure in Appendix A3. A comparison of Figures 3 and 8 reveals that both z_B* and ξ have the same functional dependence on $\phi_{B\infty}$. In addition, the $\phi_{B\infty}$'s at which ξ and z_B* reach their maxima are nearly identical. However, because of its higher N_B, system Ib has higher values of ξ than system Ia.

In addition to the strong increase in z_B*, the interfacial tension γ_{ABC} decreases rapidly as $\phi_{B\infty}$ initially increases as demonstrated in Figure 5 and Table 3. This behavior can be understood as follows. At low $\phi_{B\infty}$, the segregation of B to the A/B:C interface is favored because the system lowers its free energy by replacing more unfavorable A−C contacts with less unfavorable A−B ones. As a result γ_{ABC} decreases very rapidly. As $\phi_{B\infty}$ continues to increase, γ_{ABC} decreases much more slowly. This transition correlates with a reduction in free energy gain upon further replacing A−C contacts by A−B ones at high $\phi_{B\infty}$'s. This transition in γ_{ABC} occurs at nearly the same value of $\phi_{B\infty}$ at which z_B* is a maximum.

As mentioned earlier in this paper, in addition to reducing the interfacial tension, polymeric compatibilizers improve the mechanical properties of a blend by increasing the interfacial strength. For strongly immiscible A/C blends, we now show that the addition of a high molecular weight B component can accomplish this task. In general, an interface between incompatible phases can be strengthened if the interfacial width becomes comparable to the entanglement distance given by

$$w_{e,k} = a_k \left(\frac{M_{e,k}}{M_{0,k}} \right)^{1/2} \tag{3}$$

where a_k, $M_{e,k}$ and $M_{0,k}$ are the segment length, the entanglement molecular weight, and the monomer molecular weight of polymer k, respectively. Fetters and co-workers[29] showed that for a variety of polymers $M_{e,k}$ is given by

$$M_{e,k} = K p_k^{\,3} \rho_k \tag{4}$$

where p_k and ρ_k are the packing length and density, respectively. K is temperature dependent and has a value of *ca.* 226 A^{-3} mol^{-1} at 413 K.[29] Introduced by Witten, Milner, and Wang,[30] the packing length reflects the number of individual chains per unit volume

$$p_k = \frac{M_{0,k}}{a_k^{\,2} \rho_k N_A} \tag{5}$$

where N_A is Avogadro's constant. The values of a_k and ρ_k for polymers B and C were determined using the relations found by Strobl and Urban.[22,31] The calculated values of ρ_k, a_k, p_k, M_e, and $w_{e,k}$ for all polymers are listed in Table 4. Note that the entanglement molecular weight decreases as the mole fraction of 4-BrS increases.

A comparison of the entanglement distances with the A/B:C interfacial width provides a good indication of whether the addition of B will improve the mechanical strength. For a homopolymer/homopolymer interface reinforced with diblock copolymers, Creton and coworkers[32] reported that at least one average entanglement per block is needed for good stress transfer at the interface. The entanglement distances from Table 4 are represented by the solid lines ($w_{e,A}$), a dotted line ($w_{e,B}$), and a dash-dotted line ($w_{e,C}$.) in Figure 7. At low $\phi_{B\infty}$ (<0.2), Figure 7b shows that the A/C interpenetration (shaded region) is sufficient to produce an A/B:C interface with good mechanical strength. As $\phi_{B\infty}$ further increases, the interface strength attributed to overlap

Table 4. Entanglement Molecular Weight and Chain Statistics at 413 K[a]

symbol	N	x, y	ρ (g/cm^3)	a (Å)	p^d (Å)	$M_e{}^e$ (g/mol)	$R_0{}^f$ (Å)
A1	3844	0	1.053	6.7	3.66	11657	70.9
A2	192192	0	1.053	6.7	3.66	11657	70.9
B1	3682	0.154	1.216[b]	7.4[c]	3.07	7966	59.5
B2	6333	0.157	1.217[b]	7.4[c]	3.06	7902	59.5
C	3996	0.177	1.129[b]	7.5[c]	3.01	7060	58.3

[a] N is the number of segments, ρ is the density, a is the segment length, p is the packing length, M_e is the entanglement molecular weight, and R_0 is the square root end-to-end distance. [b] Calculated using $\rho_B = \rho_{d-PS} + 0.541x$ and $\rho_c = \rho_{PS} + 0.541y$.[22] [c] Calculated using $a_B^2 = a_{PS}^2(1 + 1.4964x)$ and $a_C^2 = a_{PS}^2(1 + 1.4964y)$.[31] [d] Calculated using eq 5. [e] Calculated using eq 4. [f] Calculated using $R_{0,k}^2 = a_k^2 N_k$.

between A and C chains is reduced because w_{AC} drops below $w_{e,A}$ and $w_{e,C}$. This reduced overlap results from the replacement of polymer C by polymer B at the interface. Whereas w_{AC} decreases, the A/B overlap increases as the B volume fraction increases. As discussed earlier, the A/B overlap increases much more strongly for system Ib because of its higher N_B. Note that at $\phi_{B\infty} = 0.2$, the A/B overlap is about equal to $w_{e,B}$ but less than $w_{e,A}$ for system Ia ($N_B = 3682$). However at the same $\phi_{B\infty}$, the A/B overlap for system Ib ($N_B = 6333$) is greater than both the B and A entanglement lengths. Thus at $\phi_{B\infty} = 0.2$, the interface should be reinforced in Ib but not Ia. By increasing $\phi_{B\infty}$ to *ca.* 0.3, system Ia should also exhibit good interfacial strength. This observation shows that the optimum concentration of B added to the system shifts to lower values as N_B increases.

Previously we showed that γ_{ABC} initially decreases rapidly with $\phi_{B\infty}$ and then more slowly for $\phi_{B\infty}$ greater than 0.30 (*cf.* Figure 5). This transition region occurs very near the $\phi_{B\infty}$ at which the interfacial width becomes comparable to the entanglement length. Thus, for the particular A/B:C system investigated in this study, the optimum compatibilizer volume fraction is *ca.* 0.30. Not surprisingly, the z_B* maxima also occur near $\phi_{B\infty} \approx 0.3$ (*cf.* Figure 3). This observation suggests that knowledge of the z_B* *vs* $\phi_{B\infty}$ behavior provides sufficient information about the optimum compatibilizer concentration in A/B:C systems. These results also demonstrate that interfacial compatibilization "efficiency" improves as N_B increases. Experiments testing the fracture toughness of the A/B:C interfaces are necessary to support these predictions. Moreover, such mechanical tests would provide important guidelines for determining the interfacial width (*i.e.*, w_{ABC}, w_{AB}, and w_{AC}) which dictates interfacial strength.

5. Conclusions

In this study, the interfacial excess of B, z_B*, was measured in a three-component, two-phase system, A/B:C, where B and C were miscible with each other but not with A. Because the A−B segmental interactions were less unfavorable than A−C ones, B was preferentially attracted to the A/B:C interface. LE-FRES was used to measure z_B*. As $\phi_{B\infty}$ increases, z_B* increases initially, reaches a maximum, and then decreases. At a given $\phi_{B\infty}$, the z_B* was found to be larger for larger values of N_B. However, z_B* was relatively insensitive to N_A. The experimental z_B*'s were compared with those calculated using the SCF model and excellent agreement was found. In addition, the SCF model was used to evaluate the interfacial tension, γ_{ABC}, the interfacial width, w_{ABC}, and the widths between the A and B (C) phases, w_{AB} (w_{AC}). Concurrent with the increase of z_B* at low $\phi_{B\infty}$, γ_{ABC} and w_{AB} were found to rapidly decrease and rapidly increase, respectively. The optimum amount of B added to the interface was found to correlate with the $\phi_{B\infty}$ producing the maximum z_B*. This optimum $\phi_{B\infty}$ also correlates with the B concentration that results in an A/B interfacial width greater than the largest entanglement length in the A/B:C system. One expects a commensurate improvement in mechanical properties as the A/B interpenetration exceeds this length. Our experimental results support the findings reported in ref 15, namely, that a small amount of high molecular weight B added to the immiscible pair of A/C can greatly enhance the interfacial properties.

Acknowledgment. This research was supported by the National Science Foundation, Division of Materials Science under Grants DMR91-58462 and DMR95-26357. This work made use of MRSEC Shared Experimental Facilities supported by the National Science Foundation under Award Number DMR96-32598. J.G. is obliged to E. J. Kramer (University of California at Santa Barbara) and K. R. Shull (Northwestern University) for useful discussions. We thank B. Rothman (The University of Pennsylvania) for his assistance with LE-FRES.

Appendix

A1. The Flory−Huggins Interaction Parameter in Poly(styrene-*co*-4-bromostyrene) Blends. The segmental interaction parameters for the two polystyrene: poly(styrene-*co*-4-bromostyrene) blends, χ_{AB} and χ_{AC}, were obtained by interpolating values from the literature.[22,23] However the interaction parameter for the blends of poly(styrene-*co*-4-bromostyrene) having different mole fractions of bromine the interaction parameter χ_{BC} was not available. This interaction parameter was determined from the rate at which the B interfacial excess increased with time. This procedure is described below.

For a binary B:C polymer blend, Jones and Kramer showed that the rate of surface segregation is diffusion limited.[33] During the growth of the surface layer, the volume fraction of the adsorbed component, B, is in local equilibrium with its volume fraction in the depleted zone adjacent to the surface, $\phi_{B\infty}'$. The surface excess of B is then

$$z_B{}^* = (\phi_{B\infty} - \phi_{B\infty}')\sqrt{D_M \tau} \qquad \text{(A1)}$$

where D_M is the mutual diffusion coefficient and τ is time. By assuming that the B interfacial excess is also diffusion controlled, we use eq A1 to extract χ_{BC}. Figure 9 shows how z_{B1}* and $\phi_{B1\infty}$ (inset) vary with $\tau^{1/2}$ at 181 °C. These results indicate that z_{B1}* increases linearly with $\tau^{1/2}$ whereas $\phi_{B1\infty}$ decreases linearly with $\tau^{1/2}$. The bulk concentration of B decreases as the interface concentration of B increase because the total amount of B in the B:C thin film must be conserved.

Using an average value of $\phi_{B1\infty} - \phi_{B1\infty}' \approx 0.0025$, the slope from eq A1 provides a measure of $D_M = 3.13 \times 10^{-14}$ cm^2/s. Using the fast theory of polymer diffusion[34] and known values of the polystyrene tracer diffusion coefficients, D*,[35] χ_{BC} was determined to be *ca.* 3.88×10^{-4}. One assumption in this calculation is that D* of

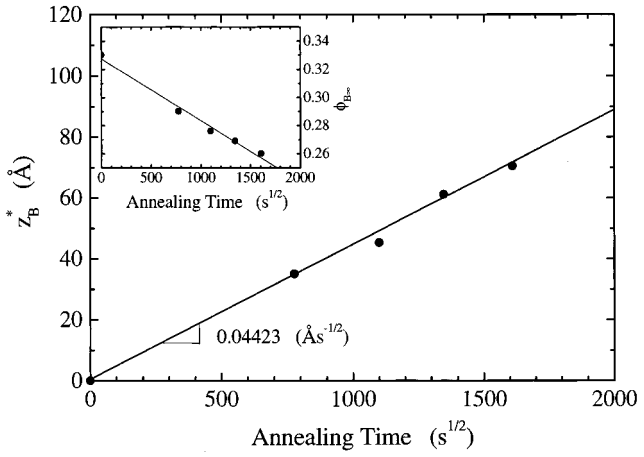

Figure 9. Interfacial excess, z_{B1}*, and bulk volume fraction of B1, $\phi_{B1\infty}$, (inset) as a function of the square root of the annealing time for system Ia. For the as-cast sample, $\phi_{B1\infty} = 0.330$.

normal PS is a good estimate for poly(styrene-*co*-4-bromostyrene) having low mole fractions of 4-BrS.

A2. The A/B:C Interfacial Tension Determined from the Gibbs Adsorption Equation. Recently, Norton and co-workers pointed out that the surface energy difference between components in binary polymer blends can be evaluated from the Gibbs adsorption equation[26]

$$d\gamma = -\sum_{(i)} \Gamma_i \, d\mu_i \tag{A2}$$

where γ, Γ_i, and μ_i are the surface tension, molecular surface excess, and chemical potential of component i, respectively. This approach was used to determine the A/B:C interfacial tension for some systems in this paper.

The interface between A and B:C phases is defined to coincide with the Gibbs dividing interface for the A component. Because $\Gamma_A = 0$ following this definition, we can write

$$\Gamma_B = -\Gamma_C \tag{A3}$$

The molecular interfacial excess is related to the interfacial excess, z_i*, of species i by

$$\Gamma_i = z_i^* \rho_i / N_i \tag{A4}$$

where ρ_i and N_i are the molar density and number of segments of i, respectively. By combining eqs A2−A4, we have

$$d\gamma = -\rho_B z_B^* \left[\frac{d\mu_B}{N_B} - \frac{d\mu_C}{N_C} \right] \tag{A5}$$

The chemical potentials, derived from the Flory−Huggins free energy,[36] are

$$\frac{\mu_B}{k_B T} = \ln \phi_{B\infty} + 1 - \phi_{B\infty} - \frac{N_B}{N_C}(1 - \phi_{B\infty}) + \chi_{BC}(1 - \phi_{B\infty})^2 N_B \tag{A6}$$

$$\frac{\mu_C}{k_B T} = \ln \phi_{C\infty} + 1 - \phi_{C\infty} - \frac{N_C}{N_B}(1 - \phi_{C\infty}) + \chi_{BC}(1 - \phi_{C\infty})^2 N_C \tag{A7}$$

where k_B is Boltzmann's constant, T is the absolute temperature, χ_{BC} is the B−C interaction parameter, and N_i and $\phi_{i,\infty}$ are the number of segments and bulk volume fraction of i, respectively. Differentiating eqs A6 and A7 with respect to the bulk volume fractions of B and C, respectively, we obtain:

$$\frac{d\mu_B}{k_B T} = \left[\frac{1}{\phi_{B\infty}} - 1 + \frac{N_B}{N_C} - 2\chi_{BC}(1 - \phi_{B\infty}) N_B \right] d\phi_{B\infty} \tag{A8}$$

$$\frac{d\mu_C}{k_B T} = \left[\frac{1}{\phi_{C\infty}} - 1 + \frac{N_C}{N_B} - 2\chi_{BC}(1 - \phi_{C\infty}) N_C \right] d\phi_{C\infty} \tag{A9}$$

Substituting eqs A8 and A9 into eq A5 yields

$$d\gamma = -k_B T \rho_B z_B^* \left[\frac{1}{N_B \phi_{B\infty}} + \frac{1}{N_C(1 - \phi_{B\infty})} - 2\chi_{BC} \right] d\phi_{B\infty} \tag{A10}$$

After integrating eq A10, the A/B:C interfacial tension relative to the A/C interfacial tension is found

$$\gamma_{ABC} = \gamma_{AC} - k_B T \rho_B \int_0^{\phi_{B\infty}} z_B^* \left[\frac{1}{N_B \phi_{B\infty}} + \frac{1}{N_C(1 - \phi_{B\infty})} - 2\chi_{BC} \right] d\phi_{B\infty} \tag{A11}$$

Equation A11 is then numerically solved using $k_B T \rho_B = 3.81$ mJ/m^2/Å, N_B, N_C, χ_{BC}, and the dependence of the experimental z_B* on $\phi_{B\infty}$.

A3. The Correlation Length of the Segregated Layer of B. Here, we describe the procedure used to determine the correlation length, ξ, from the B volume fraction profile at the A/B:C interface. First, the SCF model is used to calculate the volume fraction profiles of A, B, and C, namely, $\phi_A(x)$, $\phi_B(x)$, and $\phi_C(x)$, respectively. The position of the Gibbs dividing interface for A, x_0, is found from the condition

$$\int_{-\infty}^{x_0} [1 - \phi_A(x)] \, dx + \int_{x_0}^{\infty} \phi_A(x) \, dx = 0 \tag{A12}$$

The value of x_0 defines the origin for a new depth scale. A reduced volume fraction of B, $\phi_{B,red}(x)$, is determined from

$$\phi_{B,red}(x - x_0) = \frac{\phi_B(x)}{\phi_B(x) + \phi_C(x)} \qquad \text{for } x > x_0 \tag{A13}$$

Finally, the values of ξ are found by fitting $\phi_{B,red}(x)$ to the function

$$\phi_{B,red}(x) = \frac{\phi_{B1} - \phi_{B\infty}}{1 - \tanh\left(-\frac{h_0}{2\xi}\right)} \left[1 - \tanh\left(\frac{x - h_0}{2\xi} \right) \right] + \phi_{B\infty} \tag{A14}$$

where ϕ_{B1} and $\phi_{B\infty}$ are the volume fractions of B at the surface ($x = x_0$) and in the bulk, respectively, and h_0 is the position of the inflection point of the tanh function with respect to the origin.

References and Notes

(1) Paul, D. R., Newman, S., Eds. *Polymer Blends*; Academic Press: San Diego, CA, 1978.
(2) Utracki, L. A. *Polymer Alloys and Blends—Thermodynamics and Rheology*, Hanser Publishers: München, 1989.

(3) Helfand, E.; Tagami, Y. *J. Polym. Sci.* **1971**, *9*, 741; *J. Chem. Phys.* **1971**, *56*, 3592; *J. Chem. Phys.* **1972**, *57*, 1812.
(4) Brown, H. R. *Annu. Rev. Mater. Sci.* **1989**, *21*, 463.
(5) Xanthos, M. *Polym. Eng. Sci.* **1988**, *28*, 1392.
(6) Fayt, R.; Jerome, R.; Teyssie, P. *J. Polym. Sci., Polym. Phys. Ed.* **1989**, *27*, 775. Creton, C.; Kramer, E. J.; Hadziioannou, G. *Macromolecules* **1991**, *24*, 1846.
(7) Gersappe, D.; Irvine, D.; Balazs, A. C.; Liu, Y.; Sokolov, J.; Rafailovich, M.; Schwarz, S.; Peiffer, D. G. *Science* **1994**, *265*, 1072.
(8) Brown, H. R. *Macromolecules* **1989**, *22*, 2859.
(9) Dai, C.-A.; Dair, B. J.; Dai, K. H.; Ober, C. K.; Kramer, E. J.; Hui, C.-Y.; Jelinski, L., W. *Phys. Rev. Lett.* **1994**, *73*, 2472. Sikka, M.; Pellegrini, N. N.; Schmitt, E. A.; Winey, K. I. *Macromolecules* **1997**, *30*, 445.
(10) Noolandi, J. *Macromol. Theory Simul.* **1994**, *3*, 91. Yeung, C.; Desai, R. C.; Noolandi, J. *Macromolecules* **1994**, *27*, 55.
(11) Helfand, E. *Macromolecules* **1992**, *25*, 1676.
(12) Yoon, K.-S.; Pak, H. *Bull. Korean Chem. Soc.* **1994**, *15*, 45.
(13) Hobbs, S. Y.; Dekkers, M. E. J.; Watkins, V. H. *Polymer* **1988**, *29*, 1598.
(14) Machado, J. M.; Lee, C. S. *Polym. Eng. Sci.* **1994**, *34*, 59.
(15) Genzer, J.; Faldi, A.; Composto, R. J. *J. Chem. Phys.* **1996**, *105*, 10134.
(16) Faldi, A.; Genzer, J.; Composto, R. J.; Dozier, W. D. *Phys. Rev. Lett.* **1995**, *74*, 3388.
(17) Genzer, J.; Faldi, A.; Composto, R. J. Submitted to *Macromolecules*.
(18) Kambour, R. P.; Bendler, J. T.; Bopp, R. C. *Macromolecules* **1983**, *16*, 753.
(19) Genzer, J.; Rothman, J. B.; Composto, R. *J. Nucl. Instrum. Methods* **1994**, *B86*, 345.
(20) The fwhm values were determined from as-cast samples.
(21) Due to the long computation times, the SCF calculations were not performed for very long chain lengths, i.e., $N_A = 192\ 192$, and the following strategy was followed. Simulations were carried out for N_A's of 4000, 5000, 10 000, and 12 000. For each N_A, the corresponding values of z_B^*, γ_{ABC} and w_{ABC} were plotted as a function of $1/N_A$. By extrapolation, z_B^*, γ_{ABC}, and w_{ABC} were found.
(22) Strobl, G. R.; Urban, G. *Colloid Polym. Sci.* **1988**, *266*, 398.
(23) Bruder, F.; Brenn, R. *Macromolecules* **1991**, *24*, 5552.
(24) The error bars in Figures 3 and 4 were based only on the counting statistics in the LE-FRES spectrum. The uncertainty due to choosing the origin of the A/B:C interface was not included. At high values of $\phi_{B\infty}$, this error is particularly important. For example, if the interface shifts by 150 Å toward the B:C phase, z_B^* can be reduced by ca. 20 Å.
(25) The failure of the SCF model to produce realistic values of γ_{ABC} for system Ib (and also IIb) is not known. The model works well for all systems as $\phi_{B\infty}$ approaches 0 and 1. The model fails **at a very high N_B** and moderate $\phi_{B\infty}$, thus in the vicinity of the B:C binodal. We speculate that this close proximity of the B:C mixture to the two-phase region causes an instability in the SCF calculations.
(26) Norton, L. J.; Kramer, E. J.; Bates, F. S.; Gehlsen, M. D.; Jones, R. A. L.; Karim, A.; Felcher, G. P.; Kleb, R. *Macromolecules* **1995**, *28*, 8621.
(27) Genzer, J.; Composto, R. J. *Europhys. Lett.* **1997**, *38*, 171.
(28) de Gennes, P.-G. *Scaling Concepts in Polymer Physics*; Cornell University Press: Ithaca, NY, 1979. Binder, K. *J. Chem. Phys.* **1983**, *79*, 6387. Binder, K.; Frisch, H. L. *Macromolecules* **1984**, *17*, 2928.
(29) Fetters, L. J.; Lohse, D. J.; Richter, D.; Witten, T. A.; Zirkel, A. *Macromolecules* **1994**, *27*, 4639.
(30) Witten, T. A.; Milner, S. T.; Wang, Z.-G. In *Multiphase Macromolecular Systems*; Culbertson, B. M., Ed.; Plenum Press: New York, 1989.
(31) Strobl, G. R.; Urban, G. *J. Polym. Sci., Polym. Phys.* **1990**, *28*, 343.
(32) Creton, C.; Kramer, E. J.; Hui, C.-Y.; Brown, H. R. *Macromolecules* **1992**, *25*, 3075.
(33) Jones, R. A. L.; Kramer, E. J. *Philos. Mag.* **1990**, *B62*, 129.
(34) Composto, R. J.; Mayer, J. W.; Kramer, E. J.; White, D. M. *Phys. Rev. Lett.* **1986**, *57*, 1312.
(35) Green, P. F.; Palmstrøm, C. J.; Mayer, J. W.; Kramer, E. J. *Macromolecules* **1985**, *18*, 501.
(36) Sanchez, I. C. *Encycl. Phys. Sci. Technol.* **1992**, *13*, 153.

MA970993U